

GT2011-46140

Integrated Optimization Design for a Radial Turbine Wheel of a 100kW-Class Microturbine

Lei FU, Yan SHI, Qinghua DENG, Huaizhi LI, Zhenping FENG*

Institute of Turbomachinery, School of Energy and Power Engineering

Xi'an Jiaotong University, Xi'an 710049, P. R. China

Tel: +86-29-82665062, Fax: +86-29-82665062

E-mail: leizhenlin@gmail.com, [*zpfeng@mail.xjtu.edu.cn](mailto:zpfeng@mail.xjtu.edu.cn)

ABSTRACT

The aerodynamic performance, structural strength and wheel weight are three important factors in the design process of the radial turbine. This paper presents an investigation on these aspects and develops an optimization design approach for radial turbine with consideration of the three factors. The aerodynamic design for the turbine wheel with inlet diameter of 230mm for 100kW-class microturbine unit is carried out firstly as the original design. Then, the cylinder parabolic geometrical design method is applied to the wheel modeling and structural design, but the maximum stress predicted by Finite Element Analysis greatly exceeds the yield limit of material. Furthermore, the wheel weight is above 7.2kg thus bringing some critical difficulties for bearing design and turbine operation. Therefore, an integrated optimization design method for radial turbine is studied and developed in this paper with focus on the wheel design. Meridional profiles and shape lines of turbine wheel are optimized with consideration of the whole wheel weight. Main structural modeling parameters are reselected to reduce the wheel weight. Trade-off between aerodynamic performance and strength performance is highly emphasized during the optimization design. The results show that the optimized turbine wheel gets high aerodynamic performance and acceptable stress distribution with the weight less than 3.8kg.

NOMENCLATURE

B	Axial width of meridional view (mm)
BN	Blade numbers
D	Diameter (mm)
E	Young's modulus (GPa)
Eff	Isentropic efficiency
FEA	Finite Element Analysis
G	Mass flow rate (kg/s)
GMS	Geometrical modeling style

L	Blade height (mm)
M	Mean radius position at wheel exducer outer wall
N	Wheel rotational speed (rpm)
P	Power output (kW)
R_1	Radius of wheel exducer outer wall at hub (mm)
R_2	Radius of wheel exducer outer wall at shroud (mm)
T	Temperature ($^{\circ}\text{C}$)
TIT	Turbine inlet temperature (K)
α	Thermal expansion coefficient of material ($^{\circ}\text{C}^{-1}$)
α_1	Angle between outer endwall and radial surface (degree)
β_{bom}^0	Blade angle of mean radius at wheel exducer outer endwall (degree)
θ	Temperature range ($^{\circ}\text{C}$)
θ_{om}	Blade circumferential surrounding angle at the mean radius of wheel excuder outer endwall (degree)
Δ	Tip clearance (mm)
Δ_{m}	Blade thickness of wheel exducer outer wall at the mean radius (mm)
Δ_2	Blade thickness of the wheel exducer outer wall at shroud (mm)
Δ_4	Blade thickness of working wheel at shroud (mm)
φ_{R}	Radial angle between the pressure surface and suction surface (degree)
φ_{Z}	Axial angle between the pressure surface and suction surface (degree)
$\sigma_{0.2}$	The yield limit of material (MPa)
μ	Passion's ratio
π	Stage expansion ratio

INTRODUCTION

The microturbine has received much attention during the past decade because it is an important and useful power unit for distributed generation or distributed energy resource. Attractive features including simplicity, reliability, fast response, low emissions, and multi-fuel capabilities make the radial turbines as the ideal prime movers or key components of microturbine unit with a power range of 25-300kW [1-3]. In the previous research, several R&D works have been performed with emphasis on the aerodynamic design and strength optimization of radial turbine wheels.

For aerodynamic design of radial turbine wheel, there are several profiling generation methods. A large deflection blade design method was introduced by Tan et al [4], and it has been extended to 3-D flows and applied to a radial turbine design by Zangeneh [5]. The cylinder parabolic geometrical design method was proposed by Huang [6]. Moreover, Ebaid et al [7] described a unified approach to design a radial turbine at 60,000rpm with maximum power of 60kW electrical output.

For strength optimization of radial turbine wheel, Watanabe et al [8] presented an optimization of microturbine aerodynamics using CFD, inverse design and FEM structural analysis, and Guo [9] investigated blade vibration of a radial turbine wheel for microturbines. Xie et al [10] selected four parameters, middle inlet and outlet angle of blade, thickness in the middle of blade tip and bottom, to optimize the geometry of blade. However, the research including consideration of aerodynamic performance, structural strength and turbine wheel weight, is seldom reported.

Based on the successful research work on the designed and constructed test rig of the radial turbine for a 100kW-class microturbine unit by the TurboAero team of Xi'an Jiaotong University [10-13], the research concerning design and optimization method of turbine wheel is being continued. The work described in this paper is the second part of our R&D program. In the first part [10-13], the turbine diameter is 186mm with the rotational speed of 61,000rpm which already has been manufactured (about 3kg) and tested, and the experimental data of the turbine performances have been obtained. In the present, our program requires higher demand on the turbine design (230mm, 45,000rpm, below 4.0kg). Therefore, in this paper, an integrated optimization design method is presented and applied to optimize a radial turbine wheel with the inlet diameter of 230mm for a 100kW-class microturbine unit, in which three aspects of aerodynamic performance, structural strength and total weight of turbine wheel are taken into consideration.

ORIGINAL DESIGN

The original radial turbine design process includes two parts, that is, aerothermodynamic design and blade geometrical design. Followings are the brief descriptions about these two parts and the design results.

Aerothermodynamics design

The aerothermodynamic parameters are designed using an aerodynamic code programmed by FORTRAN, which has been developed in the TurboAero team. This program has been validated by the turbine test results to ensure its

reasonability and accuracy, thus it can be used in aerodynamic design process to achieve high performance of the turbine.

It is well known that the aerodynamic performance of state-of-the-art radial turbine is dominated by a major parameter, velocity ratio, and the peak isentropic efficiency of the radial turbine will be obtained as velocity ratio closes to 0.7. But the authors consider that the matching design between the velocity ratio and degree of reaction of the turbine is more important and must be emphasized during the design process. In this study, the velocity ratio and degree of reaction are chosen to be 0.675 and 0.45.

The basic design parameters and design target of the radial turbine for 100kW-class microturbine unit are shown in Table 1. The power and isentropic efficiency above 300kW and 80.5% are acceptable. The other aerothermodynamic design details and relative information were presented in the reference [11].

Tab. 1 Basic design parameters of radial turbine

Design Parameters	Units	Values
TIT	K	1173.15
π	-	2.96
N	r/min	45,000
G	kg/s	1.1267
D	mm	230
Δ	mm	0.5
P	kW	>300
Eff	-	>80.5%

Wheel geometrical design

The cylinder parabolic geometrical method is adopted to design the blade profiles. Because the value of profile curvature radius of parabolic modeled blade changes from large to small uniformly at the position of wheel outer wall to wheel inner wall, the flow velocity changes in flow passage is also uniform. The turbine will obtain the high efficiency as long as the reasonable meridional profiles are given.

The geometrical design method is applied using a code programmed by FORTRAN to generate the parabolic surface of the blade. The radial turbine wheel consists of two parts, the working wheel and wheel exducer. The working wheel is designed with the radial linear blade and the exducer profiles are designed by utilizing the cylinder parabolic geometrical design method, which is shown in Fig. 1. In this figure, Z is an axial length of the blade at the different radius position for the exducer. The m and n are circumferential half thickness at exducer outer and inner endwall surface.

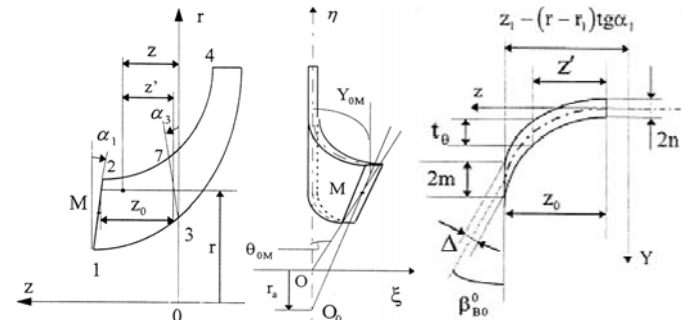


Fig. 1 Schematic diagram of geometrical design of the turbine wheel

The geometrical control parameters of the turbine wheel are presented in Table 2. More details and equations of this method can be referred to Reference [11].

The profile data of pressure surface and suction surface at hub and shroud are generated respectively, and the ruled surface of the blade is obtained. Then, the 3D geometric modeling of whole turbine wheel is generated by the CAD software and the fillet along blade root are properly modeled. The radius of fillet is linearly increased from the leading edge to trailing edge for both pressure and suction surface root.

Tab. 2 Geometrical control parameters of the turbine wheel

Control Parameters	Units	Values
Δ_4	mm	2.0
φ_Z	degree	1.0
φ_R	degree	2.0
Δ_2	mm	2.0
Δ_m	mm	2.5
α_1	degree	5.0
θ_{0m}	degree	30.0
β_{bom}^0	degree	23.0

Numerical method

To investigate the flow characteristics accurately, 3-D Navier-Stokes equations are applied in the present simulation by using commercial software NUMECA Euranus [14]. The Spalart-Allmaras one-equation turbulence model is used to represent the turbulent flow effect. The four-step Runge-Kutta algorithm is adopted to ensure numerical time integration, and an implicit residual smoothing method is used to get high CFL number. The multi-block grid is applied by the AutoGrid5 of the NUMECA with the default grid structure, and the total grid number is set to be 883,478. The grid is refined at the near-wall, endwall, leading edge, trailing edge, and tip clearance of the blade.

Flow condition is set to be the design condition, with total inlet pressure of 316.23kPa, total inlet temperature of 1,173K and inlet flow angle of 45 degree. The static pressure of 106.77kPa is defined as boundary condition at the stage outlet. Using the 3-D Navier-Stokes solver, the predicted aerodynamic performance parameters of the designed radial turbine are agreed well with that of the aerothermodynamic design in adiabatic condition. In addition, as mentioned in the introduction, the numerical methods of aerodynamic performance prediction have been validated in our past work [12], which indicated the simulation results are in good agreement with that of the experiments.

To evaluate the strength performance accurately, the commercial software ANSYS is adopted in the present simulation and the von Mises stress distribution is calculated by means of the Finite Element Analysis. Quadratic ten nodes tetrahedral mesh is used as a part of whole mesh in order to trade-off between element quality and automatic meshing with the total elements of 125,229. The refined grid used in aerodynamic computation and strength prediction is shown in Fig. 2. The rotational speed and same free displacement of the wheel outer endwall are imposed in the FEA computation.

Turbine inlet and outlet temperature are 900°C and 615°C and the temperature field is also imposed in simulation. Turbine wheel is made of a high temperature alloy with the mass density of 8,300kg/m³. At high temperature condition (900°C), Young's modulus and Passion's ratio of material are 169GPa and 0.4, respectively. Thermal expansion coefficient of material is 15.9×10⁻⁶ 1/°C. Other properties of turbine wheel material are shown in Table 3 and Table 4. The material module is imposed with these properties profiles during our calculation by using the FEA tools.

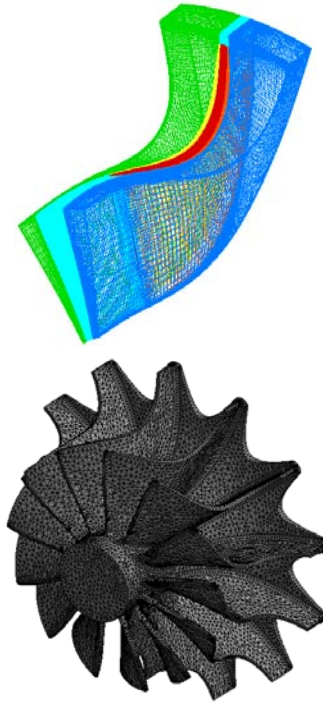


Fig. 2 Computational grids of aerodynamic and strength predictions

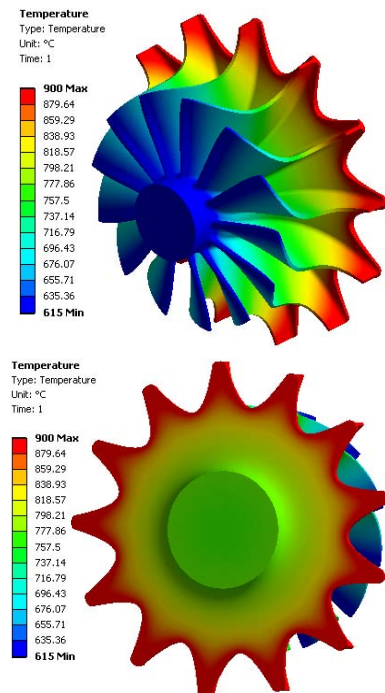


Fig. 3 Temperature field of the turbine wheel

Tab. 3 The properties of turbine wheel material

Properties	Values										
T /°C	20	100	200	300	400	500	600	700	800	900	1000
$\sigma_{0.2}$ /MPa	870	-	-	-	-	-	760	670	695	445	-
E /GPa	212	210.5	207.5	202.5	196.5	189.5	184.5	177.5	169	169	148
μ	0.31	0.31	0.35	0.34	0.33	0.36	0.42	0.39	0.37	0.4	0.4

Tab. 4 The thermal expansion coefficient of turbine wheel material

Properties	Values									
θ /°C	12~100	12~200	12~300	12~400	12~500	12~600	12~700	12~800	12~900	
$\alpha \times 10^6 / ^\circ C^{-1}$	11.8	12.2	12.7	12.8	13.5	13.9	14.6	15.1	15.9	

Results

The power and isentropic efficiency of the original design are 305kW and 89.6% respectively. The results of two major aerodynamic parameters are presented here as the reference to compare with the optimization results. This paper mainly pays attention to optimize structure and strength of the turbine wheel so that the flow details are not shown here due to the limited space. Although the overall performance of aerodynamic design meets the requirement according to the design target in Table 1, the maximum stress of 1,357MPa caused by the centrifugal force and thermal effect which is predicted by FEA already exceeds the allowable yield limit of material for turbine wheel. That means the turbine wheel should be optimized to make the strength performance satisfied the material requirements. Meanwhile, because the density of material is relatively high, the weight of whole turbine wheel is above 7.2kg. As we know, the unit shafting and bearings should sustain the wheel weight and working loads effectively, and bearings must avoid the vibration during the operation at design and off-design conditions. Obviously, this wheel weight makes the shafting and bearings design much more difficult. Therefore, the integrated optimization design considering the aerodynamic performance, structural strength and wheel weight for the radial turbine wheel is demanded in the turbine wheel design process.

INTEGRATED OPTIMIZATION DESIGN

The integrated optimization design method in this paper is divided into three steps in order to explain it clearly. However, this method is nonlinear but an iterative and repeat process with trade-off considerations among three aspects mentioned above. Figure 4 shows the flow chart of integrated optimization design which can be separated into Aerodynamics module and Structure module in general. Core steps of this optimization design method are meridional design in the aerodynamics process and blade thickness distribution in the structure modeling process. After one iteration, a new turbine wheel is worked out, and its performance analysis is obtained by numerical simulation. Then, the disadvantage of this turbine can be taken as improving guideline in next iteration. The iteration design is stopped until the new turbine wheel meets aerodynamic and strength requirements with acceptable weight synchronously.

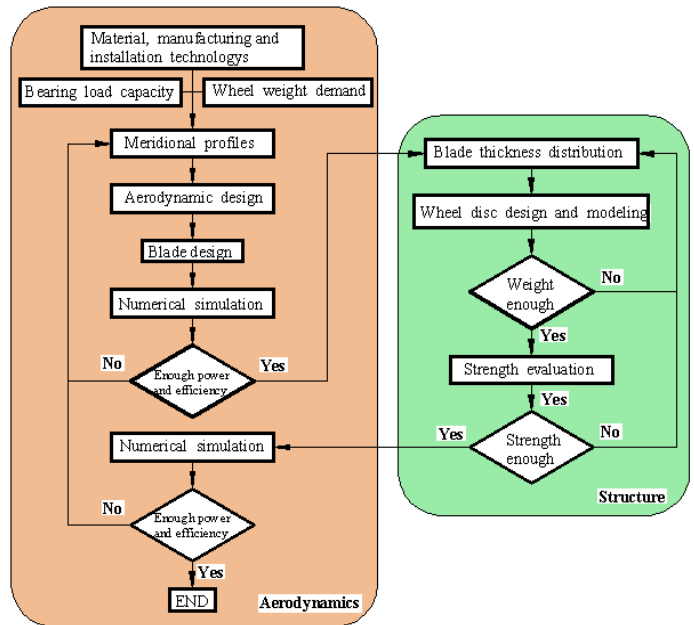


Fig. 4 Flow chart of integrated optimization design

Design and optimization steps

In general, the integrated optimization design has three steps including (1) aerodynamic design considering the wheel weight, (2) wheel geometrical design using the cylinder parabolic geometrical method which is the same as original design, and (3) 3D geometric modeling of whole turbine wheel utilizing different improvements to optimize the profiles of blade section and wheel disc. The details of these three steps are described as follows.

- (1) In the aerodynamic design process, the meridional profiles are redesigned with lower radius at the outlet of wheel exducer and the shorter width in axial direction of whole wheel. This improvement leads the cascade solidity increased, so that solid parts of whole turbine wheel decreased. In this way, the wheel weight is controlled at the beginning of radial turbine design to insure the wheel weight at the relatively low level. It should be mentioned that increased cascade solidity also leads the flow passage narrowed at the outlet of wheel exducer, and the value of flow passage width should be checked to make sure the cutting tools can enter flow passage smoothly during the manufacturing process.

- (2) In the blade geometrical design process, several geometrical control parameters are reselected according to the changes of meridional profiles. The smaller blade circumferential surrounding angle is adopted and the blade angle of mean radius at the wheel exducer outer endwall becomes larger at the same time. The profile data of pressure surface and suction surface at the hub and shroud are also regenerated by the cylinder parabolic geometrical program. In this way, the blade profiles make sure that the turbine can reach the aerodynamic requirement. The blade is still a ruled surface and has only two sections in this step.
- (3) In the 3D geometric modeling of wheel process, the wheel blade is divided into 11 cross sections from the hub to the shroud. In each cross section, profiles at pressure surface and suction surface are redistributed from the leading edge to the trailing edge. Total eleven regions of turbine wheel are refined to satisfy the strength requirement and to optimize the turbine whole weight. The blade is generated to be non-ruled surface after this step with the smoothing treatment. This step is the most complex and important step in the integrated optimization design method because the aerodynamic performance depends on blade profiles design, but the strength performance and wheel weight depends on the geometric modeling with consideration of the manufacturing and installing technology. To determine whether the required power and efficiency has been reached, an aerodynamic numerical simulation needs to be performed once the structural optimization is completed.

All numerical methods used in the optimization design of aerodynamic and strength performance predictions are the same as the original one.

Results and discussion

The differences of meridional profile are shown in Fig. 5. The first step of the integrated optimization design is to reduce the radius of outlet at wheel exducer and the meridional width to decrease the wheel weight directly. The lowest radius should make the turbine reach the aerodynamic requirements at least, which is also a trade-off result between the aerodynamic design and manufacturing demands.

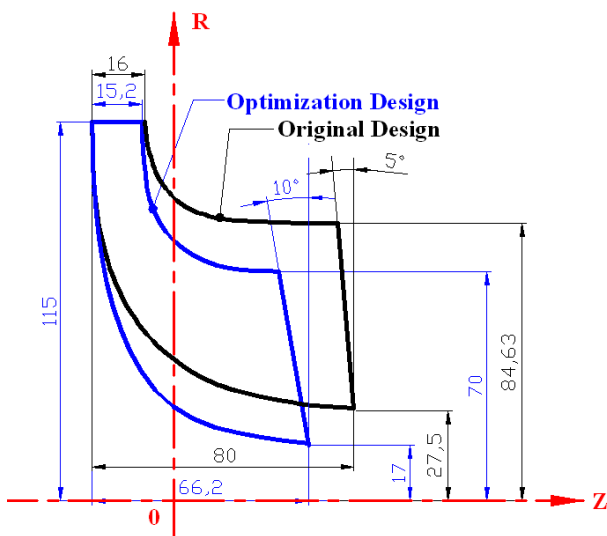


Fig. 5 The optimization of meridional profile (Step 1)

The reselected geometrical control parameters of the blade are presented in Table 5. Different parameter values between the original design and optimization design are also indicated clearly. All these changes are the second step of the integrated optimization design. Because of the increased cascade solidity, the most change is the blade circumferential surrounding angle decreased and blade angle of mean radius at the wheel exducer outer endwall increased. Angle between the exducer outer endwall and radial surface, is twice as that of original design in order to satisfy the strength requirement.

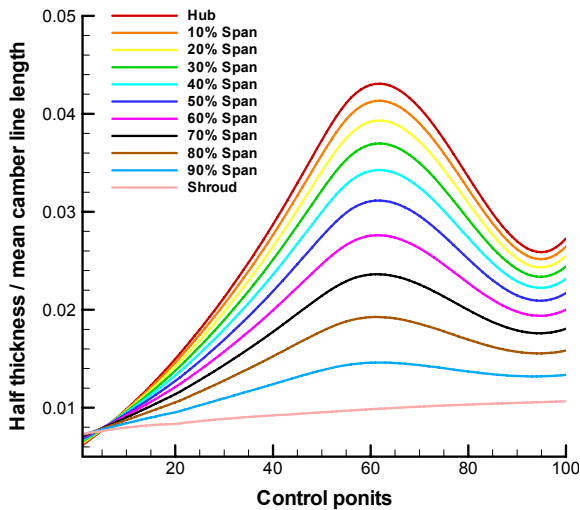
Actually, the most complex step, Step 3, includes two parts. In the first part, blade is divided into 11 cross sections in order to obtain thickness distribution in different spanwise sections. Then, the blade thickness is redistributed to modify the blade profiles and blade surface uniformly. The second part of Step 3 is the 3D geometric modeling process which focuses on the whole turbine wheel to optimize the wheel strength performance and total weight. The redistributed thicknesses of 11 blade sections are shown in Fig. 6.

Tab. 5 The optimization of geometrical control parameters (Step 2)

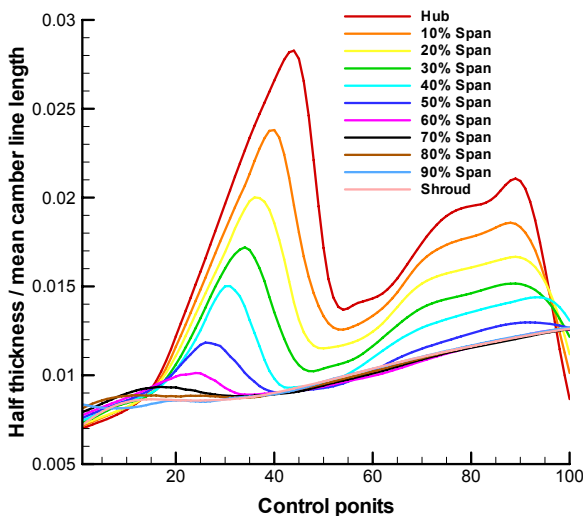
Control Parameters	Units	Original Values	Optimization Values
Δ_4	mm	2.0	3.0
φ_Z	degree	1.0	1.0
φ_R	degree	2.0	2.0
Δ_2	mm	2.0	3.0
Δ_m	mm	2.5	4.0
α_1	degree	5.0	10.0
θ_{om}	degree	30.0	20.5
β_{bom}^0	degree	23.0	39.0

In Fig. 6, the ordinate is a normalized thickness of the blade with the blade half thickness divided by the length of mean camber line. The abscissa is the number of control points along blade profile from the leading edge to the trailing edge which is total 100 points here. It is obviously that the original design has only one peak thickness region and the optimization design has two. The peak thickness regions have the different position on the blade surface in order to control the stress redistribution. On the optimized blade surface, the second peak thickness region is generated on account of the high stress region of original design. The first peak thickness region is generated for the new existing high stress region of optimized design which results from the change of meridional profile, blade profiles and geometric modeling. It is worth to note that, the quantity and position of peak thickness regions should be adjusted or regenerated for the different radial turbine design according to its own characteristic and operation condition.

In Part 1 of Step 3, the purpose is to remove the high stress region and stress concentrations area from the blade surface. It should be pointed out that peak thickness points in every blade spanwise section must be a smooth line while they connected together in the space. Failure to do so lead to much zigzag fluctuation areas on the blade surface which brings extra manufacturing difficulty in the precision casting process.



(a) Thickness distribution of original design



(b) Thickness distribution of optimization design

Fig. 6 The optimization of thickness distribution of 11 blade sections (Step 3, Part 1)

The blade modeling after smoothing treatment is shown in Fig. 7 and thicker regions on the blade surface are shown clearly. The step number and part number are also marked in the figure title to highlight every work in different step.

The second part of Step 3 is the optimization for the 3D geometric modeling of whole turbine wheel. This part has important role in the turbine wheel design which decides the wheel weight and wheel stress distribution directly. The profiles of wheel disc is redesigned to reduce the wheel mass. Therefore, the concave form of wheel backside is adopted in the optimization design process which replaces the convex form used before. Although the concave form can reduce the wheel weight, there are no high stress regions with the convex form but the concave form has. Thus, there is a trade-off design between the structural strength and wheel weight. Meanwhile, the design of concave form profiles is full of challenging. These 3D geometric modeling results and difference are shown in Fig. 8. The full view of original design and optimization design in Fig. 8 from left to right in turn includes the forward looking, back sighting, right side viewing and 3D viewing of the whole wheel.

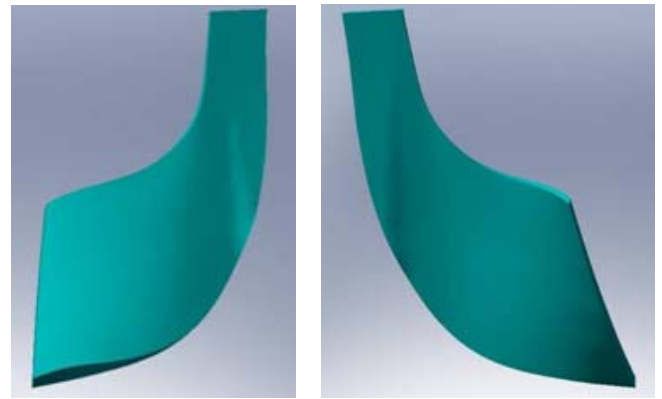


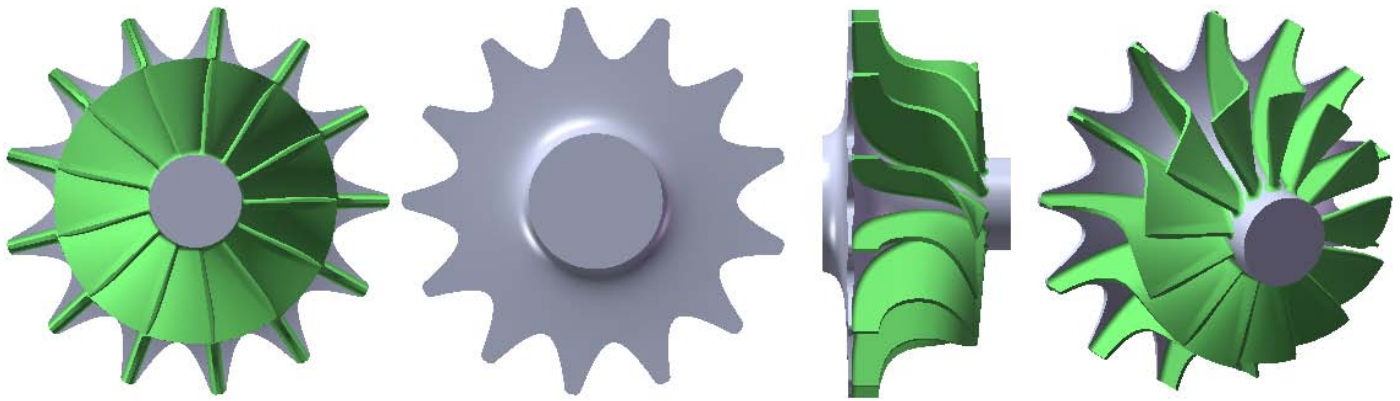
Fig. 7 The blade geometric modeling after smoothing treatment (Step 3, Part 1)

In the front view, the decrease of blade circumferential surrounding angle is obvious, so that the blade is not bounding a full flow passage due to the increased cascade solidity. The trailing edge shape is not coincident with the rotational axial any more and skews to the suction surface side which is a prerequisite condition to achieve good strength performance. The lower limit of the mass removing area for the wheel disc is not below the radius of the wheel exducer outer wall at shroud.

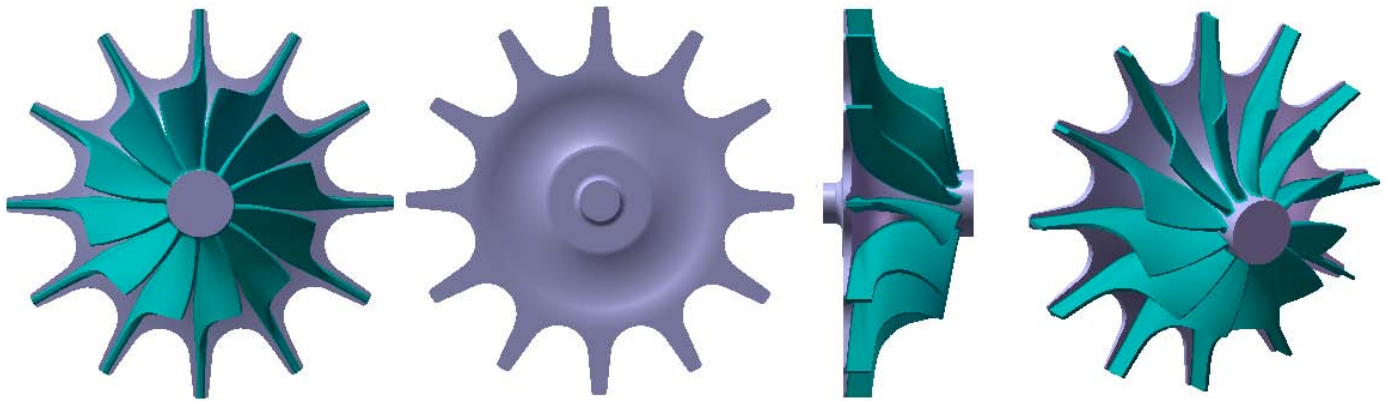
Difference of the wheel backside is the disc translating from the convex form to the concave form with several layers in order to reduce the wheel weight directly, and the surface of the wheel backsides must be translated smoothly at different radius. Different layers are connected by using the quadratic curve with each other. The radius of translating circle is not above the lower limit of mass removing area which should be noticed here. The presented concave form is designed several times to find balance between the wheel weight and strength performance.

From the right side view, the main change comes from Step 1, because the meridional profiles are redesigned. The increased cascade solidity decreases the wheel mass with reduced blade number. Even though the flow passage width located at the root of wheel exducer outlet can be smaller in theory, the minimum width of the optimization turbine is 5mm, considering the machining cost.

In Part 2, its purpose is to rebuild the stress distribution on the wheel disc backside and to remove mass of wheel as much as possible with highly considering the strength performance. Part 1 and Part 2 of integrated optimization Step 3 are both indispensable. The Part 2 is most pronounced in Step 3 because there are total eleven regions which are improved to make the strength performance and wheel weight satisfy the engineering requirements at the same time. The improved regions includes outlet edge of wheel exducer, fillet along blade root, profiles of wheel backside, mass removing for dynamic balance, and so on. After these three steps of optimization, the total weight of turbine wheel is changed from 7.2kg to 3.8kg which has 47.2% mass reduction. This is a significant improvement of the turbine wheel weight. Meanwhile, the turbine aerodynamic performance is still maintaining high power output and isentropic efficiency of 309kW and 90.8%, respectively. The details of the FEA results and strength performance of turbine wheel are analyzed subsequently.



(a) The 3D geometric modeling of original design



(b) The 3D geometric modeling of optimization design

Fig. 8 The 3D geometric modeling view of original design and optimization design (Step 3, Part 2)

A number of correction factors are considered and analyzed during the design process. Firstly, shape factor is automatically imposed throughout the geometric model by using the FEA tools. Secondly, the temperature factor is applied in our calculation by imposing the temperature field of turbine wheel. According to the yield stress limit of the turbine wheel material under different temperature, it is easy to determine whether the stress level is acceptable. In addition, the fluid pressure ranges between 43.3N-79.1N from the turbine wheel inlet to outlet on each blade. It is relatively small, and the surface effect is omitted in our calculation. In order to compare the optimization result, the calculation is only to consider the elastic deformation factor. The plastic deformation factor is not applied in our calculation even though the maximum stress exceeds the material limit in the original design.

The distribution of von Mises stress of the turbine wheel is shown in Fig. 9. According to the requirement of safe operation in engineering application, blade root fillet of the wheel is adopted and the radius is varied from the wheel inlet to outlet. The original design wheel has a high stress value of 1,261MPa located at the blade root section and pressure surface closing to the trailing edge, and the maximum stress value of 1,357MPa distributes at turbine wheel which both exceed the limitations of the material already. But the real maximum stress of turbine wheel is a bit below the calculated

stress value obtained from FEA tools. In order to compare the optimization result, this value is taken as a reference value here. The stress of other regions is acceptable with the value between 390MPa and 435MPa. After optimization, the corresponding regions has lower stress distribution except the mass removing areas with relative high stress of 478MPa. But this value does not exceed the yield limit of wheel material.

On the back of the wheel, the maximum stress of the original design has relatively lower value of 396MPa which is allowable for the turbine wheel material, and the other regions shown in the figure are more than acceptable. Corresponding to the same areas, the optimized design has higher stress distribution all over the wheel backside due to the changed disc form mentioned above. According to the yield stress limit of the turbine wheel material under local temperature, the stress level of optimized design is 504Mpa, and the yield stress limit of material is 695MPa. That means the stress is still in the allowable level. For the same reason, the maximum stress value of 530MPa on the optimized turbine wheel back is acceptable. The right picture in Fig. 9 shows the stress at the trailing edge root is already reduced from 1,261MPa to 187MPa, and the maximum stress is decreased from 1,357MPa to 598MPa in the overall level of turbine wheel. Therefore, the strength performance simulation results demonstrate that the turbine wheel has no risk in the engineering operation and applications at all.

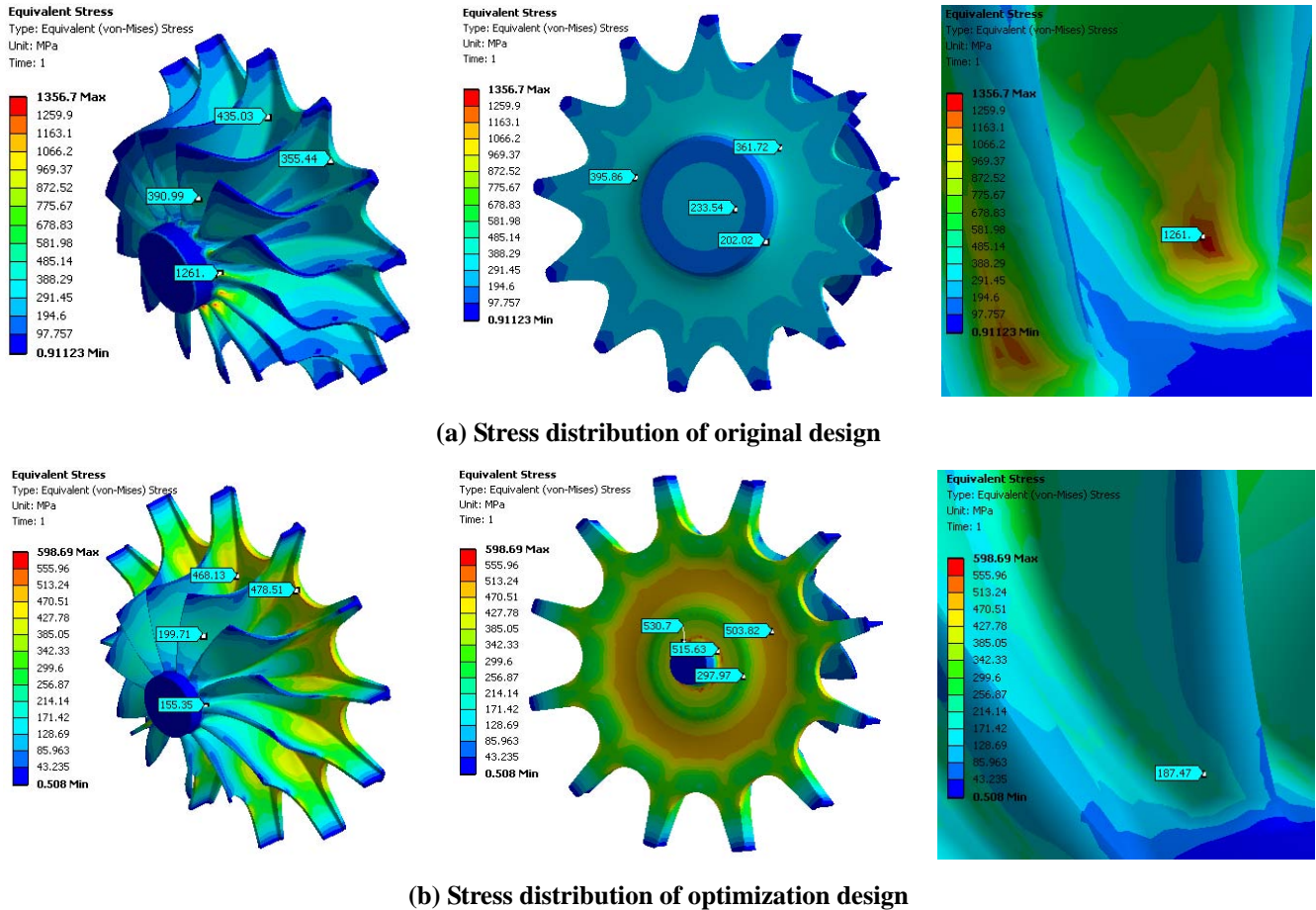


Fig. 9 The von Mises stress distribution of the turbine wheel

The local areas of turbine wheel with total eleven regions are refined to satisfy the strength requirements and to optimize the wheel weight, which are shown in Fig. 10.

In summary, Region (1) is mass removing area for dynamic balance and also for the wheel weight reduction. Mark (2) indicates the control width of the blade from the leading edge to the trailing edge. Region (3) shows the skewing trailing edge shape to the suction surface which is an essential condition to reach the well strength distribution. Mark (4) is about the high cascade solidity due to the deceased radius of the wheel exducer outer wall at the hub. Area (5) indicates the redesigned blade circumferential surrounding angle to reach high aerodynamic performance. Area (6) expresses the peak thickness position of the blade to sustain the high centrifugal stress. Mark (7) means the disc plane must be transited slightly and the fillet radius should be as small as possible in this position. Regions (8) and (9) represent the adjusted blade thickness close to the leading edge to reduce the wheel inlet horseshoe vortex and to enhance the aerodynamic efficiency. Area (10) is confirmed smooth transiting of the disc and the smoothing radius should be large as much as possible to avoid the stress concentrations. Area (11) is the final concave profiles of wheel disc backside to reduce the mass weight directly which also being a trade-off with the strength performance after several designs. With these shape optimization both in blade and turbine wheel disc, the whole integrated optimization design for turbine

wheel is accomplished in this paper and the overall performance is shown in Table 6.

Tab. 6 Performance of turbine after optimization

Parameters	Units	Original Design	Optimization Design
D	mm	230	230
R ₁	mm	27.5	17
R ₂	mm	169.3	70
L	mm	16	15.2
B	mm	80	66.2
Δ	mm	0.5	0.5
GMS	-	Ruled surface	Non ruled surface
BN	-	13	12
Mass	kg	7.2	3.8
Max. Stress	MPa	1,357	598
G	kg/s	1.1267	1.1415
P	kW	305	309
Eff	-	89.6%	90.8%

The manufacture of the optimized turbine wheel and constructions of aerodynamic performance test rig have been done. The experiments of optimization turbine will be carried out in the future to obtain the turbine performances and to validate the reliability of the integrated optimization design method.

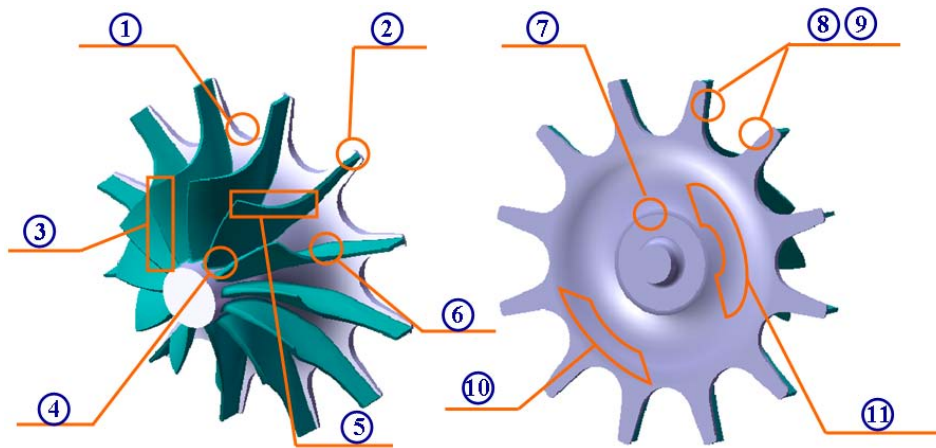


Fig. 10 Different optimization regions of the turbine wheel

CONCLUSIONS

The investigations on the aerothermodynamic design, blade geometrical design, structural strength design, wheel weight design, and CFD analysis results of a turbine wheel with inlet diameter of 230mm for 100kW-class microturbine, are conducted and presented in this paper.

To establish the turbine wheel design method and its flow chart with consideration of the material characters, shafting and bearing load capacity, manufacturing and installation technology, an integrated optimization design method including three steps to optimize aerodynamic performance, structural strength performance and wheel weight is developed and discussed in detail.

After the integrated optimization design, the turbine wheel maintains high aerodynamic performance with power output and isentropic efficiency of 309kW and 90.8%. The maximum stress of turbine wheel decreases from 1,357MPa to 598MPa, and the turbine wheel weight decreases from 7.2kg to 3.8kg. By employing this integrated optimization design method, we made the radial turbine wheel design successful and effective, which has been distinctly proven for reducing weight and improving strength performance of the turbine wheel at the same time without any noticeable degradation in turbine efficiency.

ACKNOWLEDGMENTS

The research work was sponsored by the National High Technology Research and Development Program of China - "The 100kW-class Microturbine Unit and its Energy Supply System" (No.2008AA050501).

REFERENCES

- [1] Rodgers, C., 2000, "25-5kW Microturbine Design Aspects," ASME Paper 2000-GT-0626.
- [2] Brun, K., Mckee, R. J., Moore, J., et al., 2005, "Prototype Development of A Novel Radial Flow Gas Turbine," ASME Paper GT-2005-68016.
- [3] Feng, Z. P., 2001, "Microturbine Technology and Application," Gas Turbine Power Generation Technology, 3(1), pp.9-16.

- [4] Tan, C. S., Hawthorne, W. R., McCune, J. E., et al., 1984, "Theory of Blade Design for Large Deflections: Part II —Annular Cascades," ASME Journal of Engineering for Gas Turbines and Power, 106, pp.354-365.
- [5] Zangeneh M., 1991, "A Compressible Three Dimensional Blade Design Method for Radial and Mixed Flow Turbomachinery Blades," Int. J. Numerical Methods in Fluids, 13, pp.599-624.
- [6] Huang, X. C., 1981, "Cylindrical Parabola Curve Blade Shaping Calculate of Radial Impeller and Mathematics Equation," National Defense Industry Publisher, Beijing.
- [7] Ebaid, M. S. Y., Bhinder, F. S., Khadiri, G. H., and Ei-Hasan, T. S., 2002, "A Unified Approach for Designing a Radial Flow Gas Turbine," ASME Paper GT2002-30578.
- [8] Watanabe H., Okamoto H., Guo S., Goto A. and Zangeneh M., 2004, "Optimization of Microturbine Aerodynamics using CFD, Inverse Design and FEM Structural Analysis (2nd Report, Turbine Design)," ASME Paper GT2004-53583.
- [9] Guo S., 2004, "Blade Vibration of Radial Micro Gas Turbines," The 10th International Symposium on Transport Phenomena and Dynamics of Rotating Machinery, Paper ID Number: 097.
- [10] Xie, Y. H., Deng, Q. H., Zhang, D., Feng, Z. P., 2005, "Strength Design and Numerical Analysis of Radial Inflow Turbine Impeller for A 100kW Microturbine," ASME Paper GT2005-68302.
- [11] Feng, Z. P., Deng, Q. H., Li, J., 2005, "Aerothermodynamic Design and Numerical Simulation of Radial Inflow Turbine Impeller for a 100kW Microturbine," ASME Paper GT2005-68627.
- [12] Deng, Q. H., Niu, J. F., Mao, J. R., Feng, Z. P., 2007, "Experimental and Numerical Investigation on Overall Performance of a Radial Inflow Turbine for 100kW Microturbine," ASME Paper GT2007-27707.
- [13] Deng, Q. H., Niu, J. F., Feng, Z. P., 2007, "Tip Leakage Flow in Radial Inflow Rotor of a Microturbine with Varying Blade-Shroud Clearance," ASME Paper GT2007-27722.
- [14] NUMECA International, 2006, "NUMECA FINE/Turbo Version 7.2-1".